Quaternary Research 80 (2013) 545–551

Contents lists available at ScienceDirect

Quaternary Research

journal homepage: www.elsevier.com/locate/yqres

Binary sources of loess on the Chinese Loess Plateau revealed by U–Pb ages of zircon

Xudong Che, Gaojun Li *

MOE Key Laboratory of Surficial Geochemistry, Department of Earth Sciences, Nanjing University, 163 Xianlindadao, Nanjing 210046, China

ARTICLE INFO

Article history:
Received 1 January 2013
Available online 22 August 2013

Keywords:
Loess
Detrital zircon
U–Pb ages
Provenance
Asian dust

ABSTRACT

The age distribution of detrital zircon has been used to trace sediment sources. Existing datasets show great similarity of zircon ages between the loess on the Chinese Loess Plateau (CLP) and the sediments from the North Tibetan Plateau (NTP), implying that eolian dust is delivered from the NTP to the CLP by westerly winds or via the Yellow River. However, NTP dust can also be transported by northwesterly winds from the Alxa arid lands (AALs), where materials are received from both the NTP and the Gobi Altay Mountains (GAMs). Here we report U–Pb zircon ages for AALs sands and NTP and CLP loess. The results show that the zircons in the AALs are mixed from NTP and GAMs zircons. NTP loess is mainly derived from local sources. Mixing of materials from the NTP and GAMs defines the zircon ages of the loess on the CLP better than the pure NTP source. No temporal and spatial heterogeneities of zircon ages have been observed for the loess on the CLP, which suggests that the well-mixed materials in the AALs likely have an eolian source.

Introduction

Asian dust is one of the most important components of global dust inventory (Engelbrecht and Derbyshire, 2010). Deposits of Asian dust provide valuable archives for paleo-environmental changes (e.g., Rea et al., 1998). There has been extensive research on the Chinese Loess Plateau (CLP), where massive eolian deposition began at least by the Late Oligocene (Heller and Liu, 1982; Sun et al., 1998; Guo et al., 2002; Ge and Guo, 2010; Qiang et al., 2011). Many of the paleo-proxies developed for the eolian deposits on the CLP assume either a stable dust provenance or regular source shift in response to climate changes (Zhou et al., 1990; Lu and An, 1998; Prins et al., 2007; Yang and Ding, 2008). Chemical proxies that reflect pedogenic alternation or eolian sorting have been developed assuming an unchanging composition of the primary dust, and thus a stable source region (e.g., Chen et al., 1999). The use of grain size as a proxy for wind strength also has assumed a stable source, although a variable provenance and thus the distance from the source desert would exert a strong control on the grain-size composition of the eolian deposits (e.g., Yang and Ding, 2008). Thus, source research is critical to understanding the paleo-proxies developed for the loess deposits.

Unlike other places of the world, loess on the CLP has no obvious or direct connection to glaciations (Smalley, 1995). It was thought that the arid lands from which the dust is emitted are not effective producers for silt particles (Smalley, 1995). However, more recent researches have shown that sandy lands are effective sources of silt produced by saltation and abrasion of sand grains (Crouvi et al., 2010, 2012). Thus, how the large volume of silt particles in the loess is created has been vigorously debated. Deciphering the source regions of the loess on the CLP may help to identify the mechanism that produces the silt particles (Li et al., 2009).

The grain size and dust-accumulation rate of the CLP loess both decrease gradually from northwest to southeast. Accordingly, Liu (1985) inferred a dust source in the vast arid lands to the north and northwest of the CLP. Since then, many studies have attempted to locate specific source regions (Bowler et al., 1987; Liu et al., 1994, 1996; Derbyshire et al., 1998; Ji et al., 1999; Sun, 2002; Yang and Ding, 2008). Based on geochemical and mineral tracers, several recent studies (Chen et al., 2007; Li et al., 2007; Sun et al., 2008; Li et al., 2009; Chen and Li, 2011) seem to have reached a similar conclusion that the Alxa arid lands (AALs, Fig. 1) are the major eolian provenance with material ultimately eroded from the North Tibetan Plateau (NTP) and the Gobi–Altay Mountains (GAMs). This is supported by modern meteorological observations, which show the AALs as one of the centers of dust-storm activity in northern China (Sun et al., 2001; Wang et al., 2004). The prevailing near-surface winds during the dusty season enable a southeastward transportation of dust from the AALs to the CLP (Wang et al., 2004).

However, the view of AALs as the main provenances for the loess on the CLP has been recently challenged by evidence from U–Pb ages of detrital zircon (Pullen et al., 2011; Xiao et al., 2012; Stevens et al., 2013). The rapidly developed U–Pb dating technique based on laser ablation of single zircon grains provides a new opportunity to explore the source of loess (Stevens et al., 2010; Pullen et al., 2011; Xiao et al., 2012; Xie et al., 2012). Zircon is quite stable in the earth

* Corresponding author.
E-mail address: ligaojun@nju.edu.cn (G. Li).

0033-5894/$ – see front matter
http://dx.doi.org/10.1016/j.yqres.2013.05.007

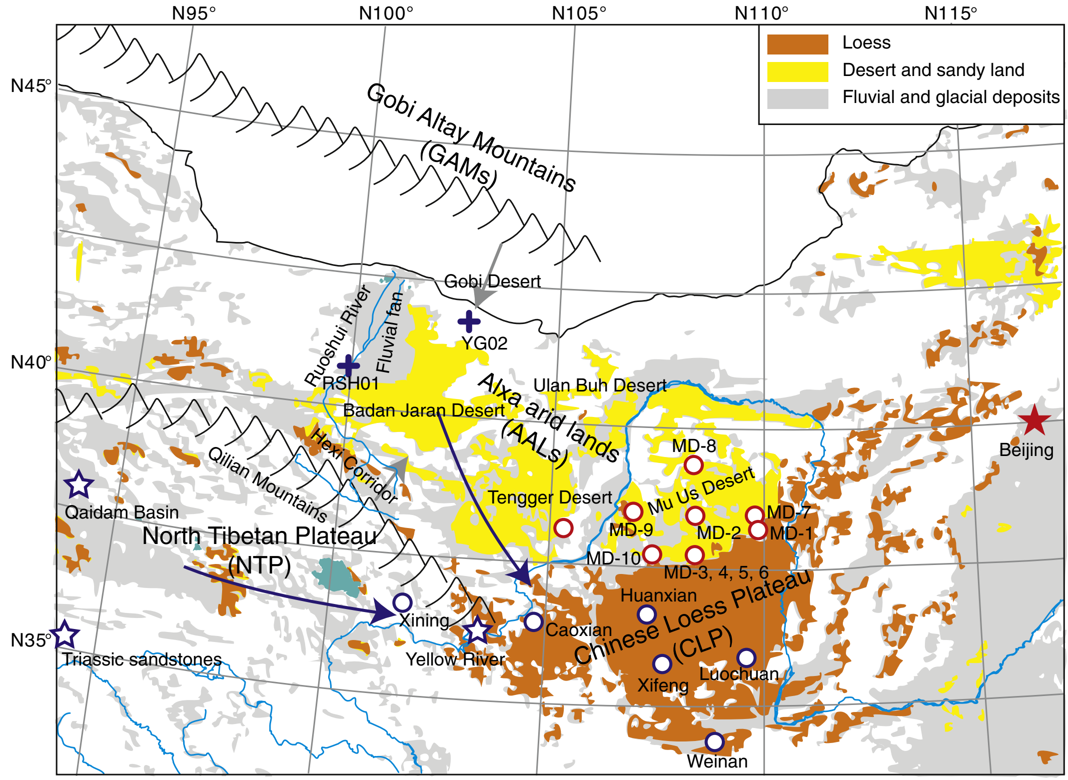

Figure 1. Map of geographic setting and sampling sites. Arrows indicate possible routes of dust transport. Also shown are locations of the samples with published zircon ages: sand in the Tengger Desert and the loess in the Huanxian site (Stevens et al., 2010); loess in the Luochuan site, the Triassic sandstones in North Tibetan Plateau, and the lacustrine sediments in Qaidam Basin (Pullen et al., 2011); loess and paleosols in the Xining, Xifeng, and Weinan sites (Xiao et al., 2012); sands and bedrock from the Mu Us Desert and the sediments in the Yellow River (Stevens et al., 2013). Blue open circles show the loess sites; red open circles are desert sands from Tengger and Mu Us Desert (Stevens et al., 2010, 2013); crosses are fluvial sand in Alxa arid lands; open stars are sediments on North Tibetan Plateau.

surface environment so that the U–Pb isotopic system within it is closed. Compared to the average signal provided by bulk geochemistry, the age population of detrital zircon grains can reflect the multiple stages of rock formation in the source regions, and thus is more diagnostic in resolving mixed sources. The contrasting geological settings of the deserts and sandy lands in northern China generate very different zircon ages for the surface sands, which could be employed to discriminate the potential source areas of loess (Stevens et al., 2010). Xie et al. (2007, 2012) have applied this technique to trace the provenance of the sand in the sandy lands and the associated loess deposits in northeastern China. Together with Hf isotopic composition, the ages of zircon indicate the Central Asian Orogenic Belt and the North China Craton as the main sources for the sandy lands and loess deposits in northeastern China (Xie et al., 2007, 2012), which is consistent with the results based on Nd and Sr isotopic compositions (Chen and Li, 2011).

Tracing the source of loess on the CLP using the U–Pb ages of zircon is more complicated. An initial study based on 84 grains from Huanxian (Fig. 1) shows that the zircon ages of loess are not similar to those of any desert samples analyzed (Stevens et al., 2010). Pullen et al. (2011) conducted extensive research on the NTP and the loess at Luochuan, finding that the zircon ages of the CLP loess share similar probability peaks with the NTP sediments. This work renewed the hypothesis that the NTP, mainly the Qaidam Basin, is the major source for the CLP loess (Bowler et al., 1987). The Qaidam Basin was recognized as a possible source due to the widespread Yardangs landforms that are creased by the eolian erosion of the lacustrine sediments there. Eolian activities with possible link to westerly winds have been observed in the Qaidam Basin and Qinghai Lake in its east (F. An et al., 2012; Z. An et al., 2012). However, the suggested transportation of dust from NTP to CLP by westerly winds implies a very different pattern of atmospheric circulation from the northwesterly winds that have been constrained by meteorological observation (Wang et al., 2004) and other source tracers (Li et al., 2009). To explain this, Pullen et al. (2011) proposed that the storm tracks might have shifted from the Alxa region during interglacial times to the NTP during glacial times due to the southward shift of westerly jet.

The NTP materials deposited on the CLP may not be derived directly from the arid lands on the NTP, but instead from adjacent regions that receive sediments fluvially from the NTP. A recent study shows that the sands in western Mu Us Desert and the Yellow River have zircon ages that are similar to those from the CLP loess, which implies that NTP materials were delivered to the CLP by the Yellow River and associated systems (Stevens et al., 2013). As suggested by Nd and Sr isotopic compositions, the NTP materials may also be indirectly derived from the AALs, that is transported from the NTP to the AALs and then to the CLP (Li et al., 2009, 2011).

Complexity arises from the spatial and temporal heterogeneities of zircon ages for the CLP loess deposits (Xiao et al., 2012), which imply multiple source regions. It has been suggested that variable mixing of dust from the NTP and the AALs may explain the spatial and temporal pattern of the zircon age population (Xiao et al., 2012). However, the evidence for the temporal and spatial heterogeneities are based on samples from only five sites on the CLP, with <100 ages for most of the samples (Xiao et al., 2012). The small sample size may introduce large statistical uncertainties.

The uncertainties associated with the source tracing of loess using zircon ages is largely due to the lack of data. One of the most likely source regions (Li et al., 2009), the AALs has only 86 zircon ages from a single sample from the Tengger Desert (Stevens et al., 2010). Thus, it is unclear whether the conclusion that the AALs are a main dust source for the CLP loess still stands in the light of new evidence from zircon ages. It is also unclear if the zircon grains with age distributions similar to those of NTP materials can be derived from the AALs, and if the contribution of Gobi dust from the AALs can explain the spatial and temporal heterogeneities of zircon ages for the loess on CLP. The present work provides new data to constrain the U–Pb ages of the zircon grains in the AALs. More data are also provided for the loess on the CLP as well as the loess on the NTP. With the help of new dataset, we concluded that the CLP loess is most likely derived from the AALs.

Samples and method

Samples

The AALs defined here are located on the low lands between the NTP and the GAMs (Fig. 1). It includes the Gobi Desert, the giant fluvial fans on the lower reach of the Ruoshui River, the Badain Jaran Desert, the Hexi Corridor, the Tengger Desert, and the Ulan Buh Desert (Fig. 1). The AALs receive debris mainly from the GAMs in the north and the NTP in the south via fluvial systems (Li et al., 2011). For the materials from the GAMs, a sample of fluvial sediment (YG02; N 41.7°, E 103.1°) from the south flank of the GAMs was used. Sediments from the bed of Ruoshui River were collected (RSH01, N 40.4°, E 99.6°) representing a mixture of materials from the NTP and the GAMs. The Ruoshui River is the largest river originating from the north flank of the Qilian Mountains. NTP materials dominate the sediments in Ruoshui River (Li et al., 2011). However, material contribution from the GAMs cannot be avoided due to the eolian transportation of Gobi dust to the catchment (Fig. 1). This is evidenced by Nd–Sr isotopes, which show that the surface sand in AALs is a mixture of the materials from NTP and GAMs (Li et al., 2011).

Samples of loess deposited during last glacial period (L1 layer) were collected in Xining (N 36.65°, E 101.74°), Caoxian (N 36.35°, E 104.62°), and Xifeng (N 35.78°, E 107.78°) (Fig. 1). Xifeng and Caoxian are on the CLP; Xining is on the eastern NTP. One paleosol sample deposited during the last interglacial period (S1 layer) was also collected from the Xifeng site.

Zircon U–Pb dating

Nonmagnetic heavy minerals were extracted from the bulk loess samples and silt fraction (<75 μm) of the two fluvial sediments by standard density liquid and magnetic separation procedures. Zircon grains were subsequently picked under a binoscope from the nonmagnetic heavy minerals. The picked zircon grains were mounted in hard resin on glass slides and polished for analysis. Cathodoluminescence images and photomicrographs of zircon grains were taken, in order to make sure that the zones of zircon for U–Pb dating are fresh and homogenous without inclusions and cracks. The analyzed zircon grains are colorless to light yellow, approximately 40–80 μm long, rounded to columnar euhedral. The oscillatory patterns on cathodoluminescence images and high Th/U ratios (>0.2) of zircon analyzed in our work indicate that most of the zircon grains are magmatic in origin.

U–Pb zircon dating was carried out at State Key Laboratory for Mineral Deposits Research, Nanjing University, by using a New Wave laser ablation system (213 nm) coupled to an Agilent 7500a quadrupole-based, inductively coupled plasma mass spectrometer (LA–ICP–MS). A 25 μm laser spot size was used at 5 Hz repetition rate with energy of 25–30 J/cm^2. In all cases, background measurement before ablation lasted 40 s, and laser ablation dwell time was 60–80 s depending on the quality of the signal. Repeated measurements of external zircon standard GEMOC GJ-1 (608.5 ± 15 Ma, Jackson et al., 2004) were used to correct for instrumental mass bias and depth dependent inter-element fractionation of Pb, Th, and U. The analytical accuracy was checked using a Mud Tank zircon standard (732 ± 5 Ma, Black and Gulson, 1978), and shows an average age of 723 ± 14 Ma (n = 24), which is consistent within 1σ of the reference age. Detailed analytical procedures are similar to Jackson et al. (2004). Common Pb was corrected using the method proposed by Andersen (2002). The $^{206}Pb/^{238}U$ age was used for grains dated as ≤1.1 Ga, and the $^{207}Pb/^{206}Pb$ age was used for grains > 1.1 Ga. Ages were rejected if discordance exceeded 10%. All accepted ages are attached in the supplementary dataset online.

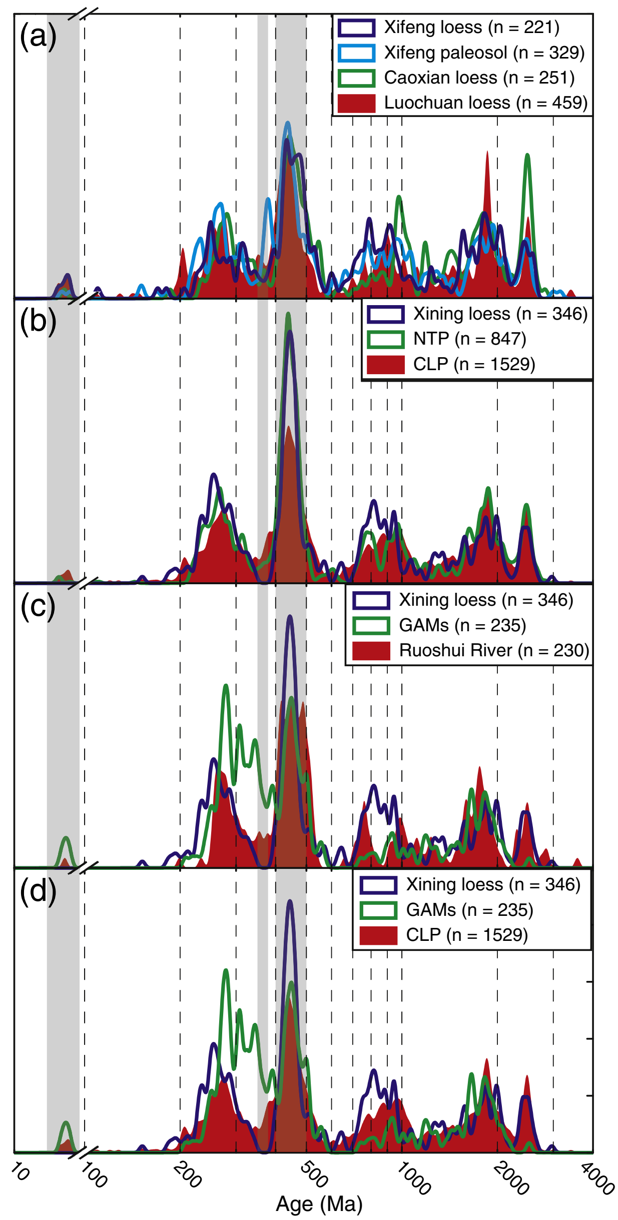

Figure 2. Kernel density plots of the zircon U–Pb ages. (a) The loess and paleosol from Caoxian and Xifeng compared with loess from Luochuan (Pullen et al., 2011); (b) the loess from Xining compared with the materials from the North Tibetan Plateau (NTP) and the loess on the Chinese Loess Plateau (CLP); (c) the sediments from the Ruoshui River and the Gobi Altay Mountains (GAMs) compared with the Xining loess; (d) CLP loess compared with Xining loess and the materials from the GAMs. Materials from the NTP are based on the average of the Yellow River sediment, the Pliocene–Pleistocene lacustrine sediment in Qaidam Basin, and the Triassic sandstones on the NTP (Pullen et al., 2011; Stevens et al., 2013). Average of loess on the CLP is based on the data from Huanxian, Luochuan, Weinan, Xifeng, and Caoxian sites (this work; Stevens et al., 2010; Pullen et al., 2011; Xiao et al., 2012). Note that the Xining and Xifeng curves have incorporated the previously published dataset (Xiao et al., 2012).

Statistical treatment

As recommended by Vermeesch (2012), the distributions of zircon ages are visualized based on Kernel density estimation (Fig. 2). A moving Gaussian window with 2% width is used to generate the Kernel density on a logarithmic time scale. Given a set of n measurements x_i $(i = 1 \ldots n)$ of one sample, the Kernel density estimator can be written as follows:

$$K(x) = \frac{1}{n}\sum_{i=1}^{n}\left\{\frac{1}{\sqrt{2\pi\sigma^2}}\exp\left[-\frac{(\ln(x)-\ln(x_i))^2}{2\sigma^2}\right]\right\} \quad (1)$$

where σ is the 'bandwidth' of 2%. The total areas of the density plots are the same for every sample on the logarithmic time scale.

Multi-sample comparison of the detrital ages could be done directly from the density plots. However, this is not convenient when the number of the samples is large. One way to visualize the similarities/dissimilarities between the age distributions is using a statistical technique called multidimensional scaling (Vermeesch, 2013). Based on a table of pairwise dissimilarities between samples, multidimensional scaling produces a two-dimensional plot of points on which similar samples cluster closely together. The distances between the points in the two-dimensional plot are proportional to the dissimilarities between the samples. Mixing samples sit approximately on the lines connecting the mixing endmembers.

Vermeesch (2013) used the Kolmogorov–Smirnov test to construct the matrix of dissimilarities. The Kolmogorov–Smirnov test calculates the absolute value of the maximum difference between the empirical cumulative distribution functions of the samples, and thus is most sensitive to the major mode of the distribution. However, the distributions of zircon ages are multimodal and different modes are equally important. Here a dissimilarity based on Kernel density estimation is suggested so that different portions of the age distribution can be considered equally (Martínez-Camblor and de Uña-Álvarez, 2009):

$$\delta_{i,j} = \int\left|K_i(x) - K_j(x)\right| d\ln(x) \quad (2)$$

where $\delta_{i,j}$ is dissimilarity between sample i and j; $K_i(x)$ and $K_j(x)$ are the Kernel densities of sample i and j derived from Eq. (1) respectively. The dissimilarity fulfills the four requirements that are desirable for the multidimensional scaling (Vermeesch, 2013): 1) $\delta_{i,j}$ is independent of sample size; 2) nonnegativity, $\delta_{i,j} = 0$ if $i = j$ and $\delta_{i,j} > 0$ otherwise; 3) symmetry, $\delta_{i,j} = \delta_{j,i}$; and 4) triangle inequality, $\delta_{i,k} \leq \delta_{i,j} + \delta_{j,k}$.

Sample with small sizes may introduce large uncertainties in Kernel densities and the dissimilarities estimates also. Thus, only samples with >100 ages were used to compute and minimize the stress value of the multidimensional scaling analysis. Samples of <100 ages were effectively ignored, although they are still plotted on the multidimensional scaling map/space that is defined by the large samples (Fig. 3). The final stress value of the multidimensional scaling is 0.054, indicating a good fit (Vermeesch, 2013).

Results

The Kernel densities and the multi-dimensional scaling map of the zircon ages are plotted in Figures 2 and 3 together with the related previously published datasets (Stevens et al., 2010; Pullen et al., 2011; Xiao et al., 2012; Stevens et al., 2013). The samples share six major peaks of age population centered at <100 Ma, ~260 Ma, ~440 Ma, 900 Ma, 1800 Ma and 2500 Ma (Fig. 2). However, the relative heights of these peaks, especially for the ~440 Ma peak, vary significantly.

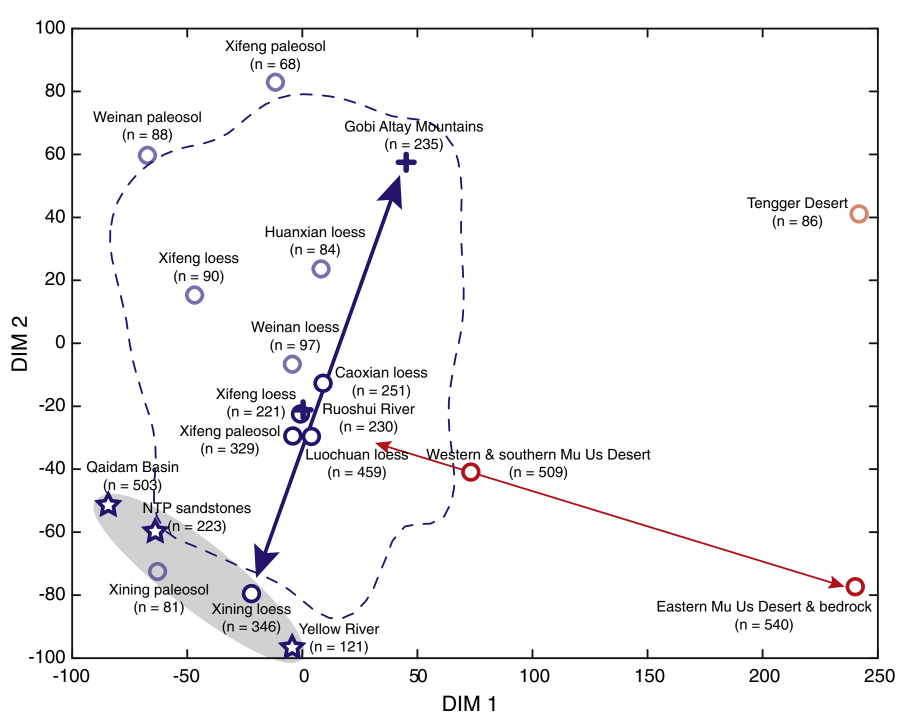

Figure 3. Multi-dimensional scaling map showing the relationship between the samples based on Kernel density statistic of the zircon ages. Arrows show possible binary mixing arrays. The symbols with faded color are data with sample size <100. Dashed line illustrate 95% range of Monte Carlo simulation by randomly resampling the loess on CLP 100 times with 100 ages each time.

Data sources: sediments eroded from the Gobi Altay Mountains, fluvial sediments in the Ruoshui River, loess from Caoxian are from this work; loess and paleosol from Xining and Xifeng (large sample size) are combined from this work and Xiao et al. (2012); loess and paleosol from Xining, Xifeng and Weinan (small sample size) are from Xiao et al. (2012); loess from Luochuan, lacustrine sediments in the Qaidam Basin, Triassic sandstones from the NTP are from Pullen et al. (2011); loess from Huanxian, sands in the western and southern Mu Us Desert (MD 3, 4, 5, 9, 10), sands and bedrock in the eastern Mu Us Desert (MD 1, 2, 6, 7, 8), sands in the Tengger Desert, and sediments in the Yellow River are from Stevens et al. (2013, 2010).

Both the density plot (Fig. 2a) and the multi-dimensional scaling map (Fig. 3) indicate that the zircon grains from the loess and paleosol layers in Caoxian and Xifeng sites share similar patterns of age distribution, which are indistinguishable from the loess in Luochuan site. However, the loess from the Xining site on the NTP has very different zircon ages than the loess on the CLP as defined by the Xifeng, Luochuan, Caoxian, Weinan, and Huanxian sites (Fig. 2b). Loess in Xining is characterized by much higher peak of age population at ~440 Ma (Fig. 2b). No zircon grain with ages <100 Ma and ~360 Ma was been detected in Xining loess (Fig. 2b). In the multi-dimensional scaling map (Fig. 3), the Xining loess shows great affinity to the NTP materials as defined by the lacustrine sediments in Qaidam Basin, the sands in the Yellow River, and the Triassic sedimentary rock on the NTP. The similarity of the zircon ages between the Xining loess and the NTP materials is also evident from nearly identical height of the ~440 Ma peak (Fig. 2b).

The two samples from the AALs show very different patterns of zircon ages (Fig. 2c). Sediments from the Ruoshui River have two distinct peaks at ~440 Ma and ~260 Ma, with the ~440 Ma peak much higher than the ~260 Ma peak. In contrast, the ~260 Ma peak and ~440 Ma peak for sediments eroded from the GAMs have similar amplitudes and are not well split due to large age population centered around 360 Ma. The <100 Ma peak of the sediments from the GAMs is higher than that of the sediments in Ruoshui river, while the 900 Ma peak and 2500 Ma peak in the GAMs sediment are not significant. The differences of zircon ages between the sediments from the Ruoshui River and the GAMs can also be seen in the multi-dimensional scaling map (Fig. 3). Ruoshui River sediment is closer to the NTP materials and is indistinguishable from the loess on the CLP (Fig. 3).

The zircon ages of the loess and the sediments in the AALs constitute a linear array in the multi-dimensional scaling map (Fig. 3). One end of the array approaches the NTP materials while another end projects to the materials eroded from the GAMs.

Discussion

Spatial and temporal heterogeneities of loess

The lack of variation between the loess and paleosol samples from Xifeng and the similar age patterns among the loess samples from the Xifeng, Caoxian and Luochuan sites is contradictory to the previous conclusion of temporal and spatial heterogeneities (Xiao et al., 2012). This is probably because the previous conclusion was based on a small dataset with sample size <100 for most of the samples (Xiao et al., 2012), and thus large statistical uncertainties. Multi-dimensional scaling analysis indicates that the previously published loess ($n = 90$) and paleosol ($n = 68$) samples from Xifeng differ from each other and also from the Luochuan loess (Fig. 3). However, with the new dataset from this study, the loess ($n = 221$) and paleosol ($n = 329$) samples from Xifeng show no difference between each other and are similar to the Luochuan loess (Fig. 3).

A Monte Carlo simulation was done to illustrate the possible statistical error introduced by small sample size. The simulation uses all the zircon ages ($n = 1529$) from the Huanxian, Luochuan, Xifeng, Weinan, and Caoxian sites on the CLP (This study; Stevens et al., 2010; Pullen et al., 2011; Xiao et al., 2012; Stevens et al., 2013). This dataset was resampled 100 times with 100 ages being randomly selected each time. The distribution of the resampled samples in the multi-dimensional scaling map is illustrated in Figure 3 by a 95% range of possibility. It shows that almost all the loess and paleosol samples with <100 ages lie within the 95% range of possibility. Thus, no conclusion of temporal and spatial heterogeneities of zircon ages can be drawn for the loess on CLP based on the existing dataset. The statistical uncertainties introduced by the small sample size may also explain why the loess samples from the small dataset are not on the mixing line between materials from the GAMs and the NTP and the large difference between the sand in Tengger Desert and the other samples in the AALs (Fig. 3).

The very similar zircon ages between the Xining loess and the NTP materials indicate that the loess in Xining is mainly derived from proximal sources on the NTP. Xining is on the eastern side of Qaidam Basin. Possible contribution of Gobi dust to the Xining loess is largely limited due to blocking by the high Qilian Mountains (Fig. 1). The prevailing westerly winds may be responsible for the transportation of NTP dust from Qaidam Basin to the Xining site (Fig. 1). Due to the extensive eolian mixing, the zircon ages of loess in Xining site may represent the average materials on the NTP.

Binary mixing of the sands in the AALs

The difference of zircon ages between the sediments in the Ruoshui River and sediments eroded from the GAMs corresponds to the geological setting of their source mountains. The GAMs are within the Central Asian Orogenic Belt. The zircon ages of the sediments from the GAMs show typical characteristics of the Central Asia Orogenic Belts with a broad age population between 200 and 600 Ma (Fig. 2c). This age population is associated with the subduction-zone magmatism during the accretion of juvenile continental crust (Bussien et al., 2011; Glorie et al., 2011). The existence of zircon with <100 Ma ages in materials from the GAMs (Fig. 2c) may reflect the widespread intra-continental magmatism in Central Asian Orogenic Belt.

The high age population at ~440 Ma for the sediments from the Ruoshui River is typical for the materials eroded from the NTP as represented by the loess in the Xining site (Fig. 2c). The Ruoshui River originates in the northern margin of Tibetan Plateau, in the Qilian Mountains (Fig. 1), where high igneous activity between 400 and 500 Ma has been inferred (Gehrels et al., 2003, 2011). However, the zircon ages of the sediments from the Ruoshui River are not exactly the same as the ages for sediment eroded from the NTP (Figs. 2c; 3). This difference can be explained by the contribution of the materials from the GAMs. Although Ruoshui River mainly drains the north flank of the Qilian Mountains and the Hexi Corridor, it carries not only the sediment eroded from the NTP but also the dust blown from the Gobi Desert — binary mixing of materials from the NTP and the GAMs in the AALs have been revealed previously by Nd and Sr isotopic compositions (Li et al., 2011). Contribution of materials from the GAMs could explain the higher age probability at ~360 Ma, the existence of <100 Ma ages, and the lower peaks at ~440 Ma and 900 Ma for the zircon in the Ruoshui River compared to the pure NTP source (Fig. 2c). The multi-dimensional scaling map also supports source mixing since the sediments in the Ruoshui River sit approximately on the line connecting the two endmembers of NTP and GAMs (Fig. 3).

Binary sources of loess

The zircon ages of loess on the CLP could be explained by a binary mixing between the materials from the NTP and the GAMs. All of the loess samples with data size >100 distribute on the hypothetical mixing array between the two endmembers of NTP and GAMs in the multi-dimensional scaling map (Fig. 3). Compared to the pure NTP source, the contribution of the materials from GAMs could explain the lower ~440 Ma peak and the existence of <100 Ma ages for the loess on CLP (Fig. 2d).

The binary mixing model suggests that both the NTP and GAMs contribute to the material budget of the loess deposits on CLP. This is consistent with the previous constraints based on isotopic tracers of Nd and Sr (Li et al., 2009). The physical erosion associated with the high terrains in the NTP and the GAMs could help to generate the massive amount of debris for the loess deposits (Smalley, 1995; Sun, 2002; Li et al., 2009). The fluvial systems associated with the high mountains transport this debris to the arid inland basins where they are subject to wind erosion and transport to the CLP. Bedrock erosion in the Mu Us Desert is not an important source for CLP loess probably because of the slow physical erosion there.

Implication for the eolian trajectories

Like the other geochemical tracers, the U–Pb ages of zircon could effectively resolve the petrological origins of the loess but not the pathway of eolian transportation. The NTP materials may be delivered to the CLP from the Qaidam Basin, the fluvial sediments associated with the Yellow River, or the AALs. For the same reason, the material from the GAMs may be lifted from the Gobi Desert or the all of the AALs where the materials from the NTP and the GAMs are mixed.

The dominant contribution of NTP materials to the loess at the Xining site suggests that arid lands on the NTP are at least a locally important source of eolian sediments (Fig. 1). However, the influence of westerly-transported NTP dust to the CLP is not clear. The interpretation depends on the average composition of the eolian dust transported from the AALs. If the average composition of the dust from the AALs approaches that of the GAMs endmember, then the contribution of the westerly-transported NTP dust to the CLP is needed to explain the data. However, the average composition of the dust from the AALs may already be similar to that of loess on the CLP due to the extensive mixing between materials from the NTP and the GAMs in the AALs. This supposition is supported by the very similar zircon ages between the sediments in the Ruoshui River and the CLP loess (Fig. 3). Thus, the contribution of the westerly-transported NTP dust to the CLP may be minor.

The lack of temporal and spatial heterogeneities of zircon ages for the loess on the CLP also implies that the AALs are the main source regions. The homogeneous compositions of zircon ages demand that the westerly-transported NTP dust and the northwesterly-transported AALs dust should be mixed in a constant ratio spatially and temporally. This may not be likely since the relative efficiencies of eolian transportation in the two source regions may change in response to glacial–interglacial climate shifts. Also, separated dust transportation would result in a higher portion of NTP material in the southwestern CLP, and a higher portion of GAMs materials in the northwestern CLP, which has not been observed by either the zircon ages of this work or the Nd and Sr isotopic tracers (Li et al., 2009). The mixing of materials from the NTP and the GAMs in the AALs thus may provide a likely explanation for the spatial and temporal homogeneities of zircon ages for the loess on the CLP.

Concerning the possible contribution of the sediments from the Yellow River (Stevens et al., 2013), we confirmed that the surface sands in the western and southern Mu Us Desert are very different from the sands in eastern Mu Us Desert and the Cretaceous sedimentary rocks that dominate the exposed bedrock of this region (Fig. 3). The sands in the western and southern Mu Us Desert do approach the CLP loess in the multi-dimensional scaling map, but differ from the Yellow River sediments. Mixing between the bedrock debris and the eolian input similar to the CLP may explain the zircon ages of the sands of the southern and western Mu Us Desert (Fig. 3). The Mu Us Desert is north of the CLP; thus, it is reasonable to assume that it receives the same eolian inputs as the CLP. Eolian input with similar composition to that of loess has also been suggested by the size dependence of Nd isotopic composition for the sediments of the Mu Us Desert (Rao et al., 2008).

Finding the binary sources for the loess on the CLP has important implications for interpreting the paleo-proxies archived in the loess deposits. Competition of the two sources reflected by the geochemical compositions of the loess deposits may record the response of past surface processes to climatic and tectonic changes (Chen and Li, 2013). Binary source mixing may also help to identify possible changes in atmospheric circulation using the geochemical tracers that show great contrast between the two endmembers. The lack of glacial–interglacial changes of zircon ages as recorded for the Xifeng site indicates that the suggested shift of storm tracks from the AALs to the NTP during the glacial periods may not have happened.

Conclusion

The new dataset of detrital zircon ages provided by this work may improve our understanding of the eolian source of the loess on the CLP. It is shown that small sample size may introduce large statistical uncertainties when comparing the zircon ages between samples. No spatial and temporal heterogeneities of zircon ages have been observed for the loess on CLP if only the samples with large sample size are considered. Loess in Xining is dominated by the westerly-transported NTP dust, and thus can be taken as representative for the average NTP materials.

A binary mixture of the materials eroded from the NTP and the GAMs fits the zircon ages of the loess on CLP better than a pure NTP source. Both the NTP and GAM signatures have been reflected by the zircon ages of the sands in the AALs since the AALs receive sediments from both the NTP and the GAMs. Thus, direct transportation of dust from the NTP to the CLP is not required to explain the NTP signatures of zircon ages in the loess on the CLP. Zircons with similar age distribution to those of the NTP could also be derived from the AALs. Instead, due to additional contribution of the materials from the GAMs, zircon grains from the AALs match the zircon ages of the CLP loess better. The binary source mixing for the CLP loess confirms the previous conclusion based on Nd and Sr isotopic constrains (Li et al., 2009; Chen and Li, 2011). The lack of temporal and spatial variations of zircon ages for the CLP favors the AALs as the main dust source. Proposed shifting of storm tracks from south from the AALs to the NTP during the glacial periods may not have happened.

Acknowledgments

We thank Zhong Chen, Tao Li, Fei Liu, Rongqing Zhang, Wenfang Zhang, and Bin Wu for assistances in the LA–ICP–MS lab. Discussions with Guoqiao Xiao and Jing Xie have improved our interpretation. Zhongping Lai (associate editor), Alan Gillespie (editor), and the two reviewers are deeply thanked for their constructive suggestions and English editing. This work was supported by National Natural Science Foundation of China (Grant no. 41102103, 41173105 and 41021002).

Appendix A. Supplementary data

Supplementary data to this article can be found online at http://dx.doi.org/10.1016/j.yqres.2013.05.007.

References

An, F., Ma, H., Wei, H., Lai, Z., 2012. Distinguishing aeolian signature from lacustrine sediments of the Qaidam Basin in northeastern Qinghai-Tibetan Plateau and its palaeoclimatic implications. Aeolian Research 4, 17–30.

An, Z., Colman, S.M., Zhou, W., Li, X., Brown, E.T., Jull, A.J.T., Cai, Y., Huang, Y., Lu, X., Chang, H., Song, Y., Sun, Y., Xu, H., Liu, W., Jin, Z., Liu, X., Cheng, P., Liu, Y., Ai, L., Li, X., Liu, X., Yan, L., Shi, Z., Wang, X., Wu, F., Qiang, X., Dong, J., Lu, F., Xu, X., 2012. Interplay between the Westerlies and Asian monsoon recorded in Lake Qinghai sediments since 32 ka. Scientific Reports 2. http://dx.doi.org/10.1038/srep00619.

Andersen, T., 2002. Correction of common lead in U–Pb analyses that do not report ^{204}Pb. Chemical Geology 192, 59–79.

Black, L.P., Gulson, B.L., 1978. The age of the Mud Tank carbonatite, Strangways Range, Northern Territory. BMR Journal of Geology and Geophysics 3, 227–232.

Bowler, J.M., Chen, K.Z., Yuan, B.Y., 1987. Systematic variations in loess source areas: evidence from Qaidam and Qinghai basins, western China. In: Liu, T.S. (Ed.), Aspects of Loess Research. China Ocean Press, Beijing, pp. 39–51.

Bussien, D., Gombojav, N., Winkler, W., von Quadt, A., 2011. The Mongol–Okhotsk Belt in Mongolia — an appraisal of the geodynamic development by the study of sandstone provenance and detrital zircons. Tectonophysics 510, 132–150.

Chen, J., Li, G., 2011. Geochemical studies on the source region of Asian dust. Science China Earth Sciences 54, 1279–1301.

Chen, Z., Li, G., 2013. Evolving sources of eolian detritus on the Chinese Loess Plateau since early Miocene: tectonic and climatic controls. Earth and Planetary Science Letters 371–372, 220–225.

Chen, J., An, Z., Head, J., 1999. Variation of Rb/Sr ratios in the loess–paleosol sequences of Central China during the Last 130,000 years and Their implications for monsoon paleoclimatology. Quaternary Research 51, 215–219.
Chen, J., Li, G.J., Yang, J.D., Rao, W.B., Lu, H.Y., Balsam, W., Sun, Y.B., Ji, J.F., 2007. Nd and Sr isotopic characteristics of Chinese deserts: implications for the provenances of Asian dust. Geochimica et Cosmochimica Acta 71, 3904–3914.
Crouvi, O., Amit, R., Enzel, Y., Gillespie, A.R., 2010. Active sand seas and the formation of desert loess. Quaternary Science Reviews 29, 2087–2098.
Crouvi, O., Schepanski, K., Amit, R., Gillespie, A.R., Enzel, Y., 2012. Multiple dust sources in the Sahara Desert: the importance of sand dunes. Geophysical Research Letters 39, L13401.
Derbyshire, E., Meng, X., Kemp, R.A., 1998. Provenance, transport and characteristics of modern aeolian dust in western Gansu Province, China, and interpretation of the Quaternary loess record. Journal of Arid Environments 39, 497–516.
Engelbrecht, J.P., Derbyshire, E., 2010. Airborne mineral dust. Elements 6, 241–246.
Ge, J.Y., Guo, Z.T., 2010. Neogene eolian deposits within the West Qinling Mountains: climatic and tectonic implications. Chinese Science Bulletin 55, 1483–1487.
Gehrels, G.E., Yin, A., Wang, X.-F., 2003. Detrital-zircon geochronology of the northeastern Tibetan plateau. Geological Society of America Bulletin 115, 881–896.
Gehrels, G., Kapp, P., DeCelles, P., Pullen, A., Blakey, R., Weislogel, A., Ding, L., Guynn, J., Martin, A., McQuarrie, N., Yin, A., 2011. Detrital zircon geochronology of pre-Tertiary strata in the Tibetan–Himalayan orogen. Tectonics 30, TC5016.
Glorie, S., De Grave, J., Buslov, M.M., Zhimulev, F.I., Izmer, A., Vandoorne, W., Ryabinin, A., Van den haute, P., Vanhaecke, F., Elburg, M.A., 2011. Formation and Palaeozoic evolution of the Gorny-Altai — Altai-Mongolia suture zone (South Siberia): zircon U/Pb constraints on the igneous record. Gondwana Research 20, 465–484.
Guo, Z.T., Ruddiman, W.F., Hao, Q.Z., Wu, H.B., Qiao, Y.S., Zhu, R.X., Peng, S.Z., Wei, J.J., Yuan, B.Y., Liu, T.S., 2002. Onset of Asian desertification by 22 Myr ago inferred from loess deposits in China. Nature 416, 159–163.
Heller, F., Liu, T.-S., 1982. Magnetostratigraphical dating of loess deposits in China. Nature 300, 431–433.
Jackson, S.E., Pearson, N.J., Griffin, W.L., Belousova, E.A., 2004. The application of laser ablation–inductively coupled plasma–mass spectrometry to in situ U–Pb zircon geochronology. Chemical Geology 211, 47–69.
Ji, J., Chen, J., Lu, H., 1999. Origin of illite in the loess from the Luochuan area, Loess Plateau, central China. Clay Minerals 34, 525–532.
Li, G., Chen, J., Chen, Y., Yang, J., Ji, J., Liu, L., 2007. Dolomite as a tracer for the source regions of Asian dust. Journal of Geophysical Research 112, D17201. http://dx.doi.org/10.1029/2007JD008676.
Li, G., Chen, J., Ji, J., Yang, J., Conway, T.M., 2009. Natural and anthropogenic sources of East Asian dust. Geology 37, 727–730.
Li, G., Pettke, T., Chen, J., 2011. Increasing Nd isotopic ratio of Asian dust indicates progressive uplift of the north Tibetan Plateau since the middle Miocene. Geology 39, 199–202.
Liu, T.S., 1985. Loess and the Environment. China Ocean Press, Beijing 1–321.
Liu, C.Q., Masuda, A., Okada, A., Yabuki, S., Fan, Z.L., 1994. Isotope geochemistry of Quaternary deposits from the arid lands in Northern China. Earth and Planetary Science Letters 127, 25–38.
Liu, T., Ding, M., Derbyshire, E., 1996. Gravel deposits on the margins of the Qinghai-Xizang Plateau, and their environmental significance. Palaeogeography, Palaeoclimatology, Palaeoecology 120, 159–170.
Lu, H.Y., An, Z.S., 1998. Paleoclimatic significance of grain size of loess–palaeosol deposit in Chinese Loess Plateau. Science in China Series D-Earth Sciences 41, 626–631.
Martínez-Camblor, P., de Uña-Álvarez, J., 2009. Non-parametric -sample tests: density functions vs distribution functions. Computational Statistics & Data Analysis 53, 3344–3357.
Prins, M.A., Vriend, M., Nugteren, G., Vandenberghe, J., Lu, H., Zheng, H., Jan Weltje, G., 2007. Late Quaternary aeolian dust input variability on the Chinese Loess Plateau: inferences from unmixing of loess grain-size records. Quaternary Science Reviews 26, 230–242.
Pullen, A., Kapp, P., McCallister, A.T., Chang, H., Gehrels, G.E., Garzione, C.N., Heermance, R.V., Ding, L., 2011. Qaidam Basin and northern Tibetan Plateau as dust sources for the Chinese Loess Plateau and paleoclimatic implications. Geology 39, 1031–1034.
Qiang, X., An, Z., Song, Y., Chang, H., Sun, Y., Liu, W., Ao, H., Dong, J., Fu, C., Wu, F., Lu, F., Cai, Y., Zhou, W., Cao, J., Xu, X., Ai, L., 2011. New eolian red clay sequence on the western Chinese Loess Plateau linked to onset of Asian desertification about 25 Ma ago. Science China Earth Sciences 54, 136–144.
Rao, W., Chen, J., Yang, J., Ji, J., Li, G., Tan, H., 2008. Sr–Nd isotopic characteristics of eolian deposits in the Erdos Desert and Chinese Loess Plateau: implications for their provenances. Geochemical Journal 42, 273–282.
Rea, D.K., Snoeckx, H., Joseph, L.H., 1998. Late Cenozoic eolian deposition in the North Pacific: Asian drying, Tibetan uplift, and cooling of the northern hemisphere. Paleoceanography 13, 215–224.
Smalley, I., 1995. Making the material: the formation of silt sized primary mineral particles for loess deposits. Quaternary Science Reviews 14, 645–651.
Stevens, T., Palk, C., Carter, A., Lu, H., Clift, P.D., 2010. Assessing the provenance of loess and desert sediments in northern China using U–Pb dating and morphology of detrital zircons. Geological Society of America Bulletin 122, 1331–1344.
Stevens, T., Carter, A., Watson, T.P., Vermeesch, P., Andò, S., Bird, A.F., Lu, H., Garzanti, E., Cottam, M.A., Sevastjanova, I., 2013. Genetic linkage between the Yellow River, the Mu Us desert and the Chinese Loess Plateau. Quaternary Science Reviews. http://dx.doi.org/10.1016/j.quascirev.2012.1011.1032.
Sun, J.M., 2002. Provenance of loess material and formation of loess deposits on the Chinese Loess Plateau. Earth and Planetary Science Letters 203, 845–859.
Sun, D.H., Shaw, J., An, Z.S., Cheng, M.Y., Yue, L.P., 1998. Magnetostratigraphy and paleoclimatic interpretation of a continuous 7.2 Ma Late Cenozoic eolian sediments from the Chinese Loess Plateau. Geophysical Research Letters 25, 85–88.
Sun, J.M., Zhang, M.Y., Liu, T.S., 2001. Spatial and temporal characteristics of dust storms in China and its surrounding regions, 1960–1999: relations to source area and climate. Journal of Geophysical Research-Atmospheres 106, 10325–10333.
Sun, Y.B., Tada, R.J., Chen, J.C., Liu, Q.S., Toyoda, S., Tani, A., Ji, J.F., Isozaki, Y., 2008. Tracing the provenance of fine-grained dust deposited on the central Chinese Loess Plateau. Geophysical Research Letters 35, L01804. http://dx.doi.org/10.1029/2007GL031672.
Vermeesch, P., 2012. On the visualisation of detrital age distributions. Chemical Geology 312–313, 190–194.
Vermeesch, P., 2013. Multi-sample comparison of detrital age distributions. Chemical Geology 341, 140–146.
Wang, X., Dong, Z., Zhang, J., Liu, L., 2004. Modern dust storms in China: an overview. Journal of Arid Environments 58, 559–574.
Xiao, G., Zong, K., Li, G., Hu, Z., Dupont-Nivet, G., Peng, S., Zhang, K., 2012. Spatial and glacial-interglacial variations in provenance of the Chinese Loess Plateau. Geophysical Research Letters 39, L20715.
Xie, J., Wu, F.Y., Ding, Z.L., 2007. Detrital zircon composition of U–Pb ages and Hf isotope of the Hunshandake sandy land and implications for its provenance. Acta Petrologica Sinica 523–528.
Xie, J., Yang, S., Ding, Z., 2012. Methods and application of using detrital zircons to trace the provenance of loess. Science China Earth Sciences 55, 1837–1846.
Yang, S., Ding, Z., 2008. Advance–retreat history of the East-Asian summer monsoon rainfall belt over northern China during the last two glacial–interglacial cycles. Earth and Planetary Science Letters 274, 499–510.
Zhou, L.P., Oldfield, F., Wintle, A.G., Robinson, S.G., Wang, J.T., 1990. Partly pedogenic origin of magnetic variations in Chinese loess. Nature 346, 737–739.